

## Quantum control of femtosecond resonance-enhanced multiphoton-ionization photoelectron spectroscopy

Shian Zhang,<sup>1,\*</sup> Chenhui Lu,<sup>1</sup> Tianqing Jia,<sup>1</sup> Jianrong Qiu,<sup>2</sup> and Zhenrong Sun<sup>1,†</sup>

<sup>1</sup>State Key Laboratory of Precision Spectroscopy, and Department of Physics, East China Normal University, Shanghai 200062, People's Republic of China

<sup>2</sup>State Key Laboratory of Luminescent Materials and Devices, and Institute of Optical Communication Materials, South China University of Technology, Wushan Road 381, Guangzhou 510640, People's Republic of China

(Received 23 May 2013; published 31 October 2013)

We establish a theoretical model based on perturbation theory to show that the resonance-enhanced multiphoton-ionization photoelectron spectroscopy (REMPI-PS) in cesium (Cs) atom can be effectively enhanced and narrowed by appropriately shaping the femtosecond laser pulse, and the corresponding physical control processes can be well illustrated by considering the inter- and intragroup interferences involving on- and near-resonant three-photon excitation pathways. Consequently, a high-resolution REMPI-PS and fine energy-level diagram of the excited states can be obtained in spite of the broad femtosecond laser spectrum.

DOI: [10.1103/PhysRevA.88.043437](https://doi.org/10.1103/PhysRevA.88.043437)

PACS number(s): 32.80.Qk, 32.80.Rm, 42.50.Md

Studying the microscopic behaviors of atom and molecule is always an interesting subject of scientists, which is very helpful for understanding and manipulating the macroscopic world. Resonance-enhanced multiphoton-ionization photoelectron spectroscopy (REMPI-PS), involving a resonant single- or multiple-photon absorption to an excited state followed by another photon that ionizes the atom or molecule, has become a powerful technique applied to the atomic and molecular spectroscopy [1–5], and has been widely applied to study the excited or Rydberg state structure and the photoionization and dissociation process [6–14]. By observing REMPI-PS, one can determine which excited state is ionized that offers the structure information of the excited states, and also identify the dynamical processes occurring in the excited states that the electrons derive from the ionization of the neutral medium or the dissociation of the parent ion.

Nanosecond or picosecond laser pulse was a well-established tool to achieve high-resolution REMPI-PS [15–18], but the nanosecond or picosecond REMPI-PS was not suitable to study the dynamical process of the excited state due to the long pulse duration, such as transient population, wavepacket evolution, proton transfer, and so on. The femtosecond laser pulse was considered as an ideal excitation source because of its high laser intensity and short pulse duration [19,20], while an inevitable question for the femtosecond REMPI-PS is poor spectral resolution due to the large laser spectral bandwidth. Recently, the advent of the femtosecond pulse shaping technique by modulating the laser spectral phase and/or amplitude in the frequency domain opened an opportunity to effectively control the femtosecond REMPI-PS. Various phase modulation schemes have been proposed to enhance or narrow the REMPI-PS [21–29], and some schemes have been experimentally realized [21–25]. For example, Wollenhaupt *et al.* experimentally demonstrated the selective excitation of the slow and fast photoelectron components of REMPI-PS by sinusoidal, chirped, or phase-step modulation [21–24]. Krug *et al.* experimentally achieved the enhancement

and suppression of REMPI-PS by chirped phase modulation [25]. We theoretically propose a  $\pi$  or cubic phase modulation to realize the enhancement and narrowing of REMPI-PS [26–29]. In theory, the photoelectron spectral modulation was explained by the selective population of dressed states [21–24], or multiphoton power spectrum [28,29].

In our previous works [26–29], the REMPI-PS was calculated by considering the laser field in time domain; thus the physical control mechanism of the photoelectron spectral modulation cannot be directly explained from this theoretical model, which greatly limits the understanding of the resonance-enhanced multiphoton-ionization process. However, in this paper we develop a theoretical model by considering the laser field in frequency domain and show that the REMPI process involves the on- and near-resonant excitation pathways, and therefore the photoelectron spectral modulation can be well explained by the inter- and intragroup interference involving these on- and near-resonant excitation pathways. Our results show that the REMPI-PS signal can be greatly enhanced and narrowed via the inter- and intragroup interferences involving on- and near-resonant multiphoton excitation pathways by properly designing the laser spectral phase, and thus a high-resolution REMPI-PS and fine energy-level diagram of the excited states can be obtained.

The  $(2+1)$  resonance-enhanced three-photon ionization process excited by the femtosecond laser field  $E(t)$  is schematically shown in Fig. 1(a); here the ground state  $|g\rangle$  and the excited state  $|f\rangle$  are coupled by a nonresonant two-photon absorption, and then the excited state  $|f\rangle$  is coupled to the ionization continuum by absorbing the other photon. In the present study, we consider this case in the perturbative regime that the light-matter interaction can be described by time-dependent perturbation theory, and thus the  $(2+1)$  REMPI-PS signal  $P^{(2+1)}(E_v)$  can be approximated as [30,31]

$$P^{(2+1)}(E_v) \propto \left| \sum_k \mu_{cf} \mu_{fk} \mu_{kg} \int_{-\infty}^{+\infty} \int_{-\infty}^{t_1} \int_{-\infty}^{t_2} E(t_1) E(t_2) E(t_3) \times \exp\{i[(E_v + E_f)/\hbar - \omega_{fg}]t_1\} \exp(i\omega_{fk}t_2) \times \exp(i\omega_{kg}t_3) dt_1 dt_2 dt_3 \right|^2, \quad (1)$$

\*sazhang@phy.ecnu.edu.cn

†zrsun@phy.ecnu.edu.cn

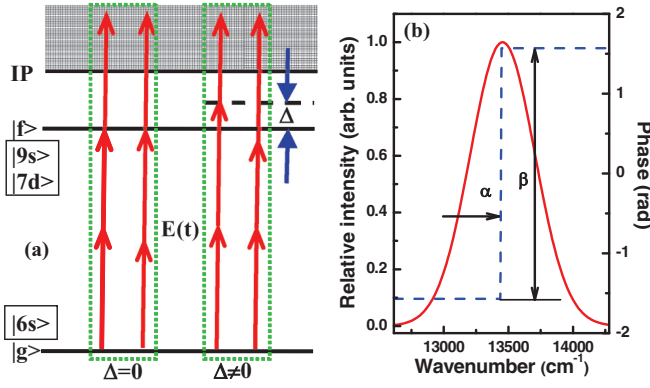


FIG. 1. (Color online) (a)  $(2+1)$  resonance-enhanced three-photon ionization process with several excitation pathways that are on resonance ( $\Delta = 0$ ) and near resonance ( $\Delta \neq 0$ ) with the excited state  $|f\rangle$ . (b) The laser spectrum is modulated by a spectral phase step modulation (blue dashed line), where  $\alpha$  and  $\beta$  respectively represent the phase step position and modulation depth.

where  $E_I$  is the ionization energy,  $\mu_{mn} = \langle m|\mu|n\rangle$  is the dipole matrix element from the states  $|n\rangle$  to  $|m\rangle$ , and  $\omega_{mn} = (E_m - E_n)/\hbar$  is the corresponding transition frequency. By transforming Eq. (1) into the frequency domain,  $P^{(2+1)}(E_v)$  can be further written as

$$P^{(2+1)}(E_v) \propto \mu_{cf} \mu_{fg}^2 |A_{\text{on-res}}^{(2+1)}(E_v) + A_{\text{near-res}}^{(2+1)}(E_v)|^2, \quad (2)$$

where  $\mu_{fg}^2$  is the effective nonresonant two-photon dipole coupling from the states  $|g\rangle$  to  $|f\rangle$ , and  $A_{\text{on-res}}^{(2+1)}(E_v)$  and  $A_{\text{near-res}}^{(2+1)}(E_v)$  are given by

$$A_{\text{on-res}}^{(2+1)}(E_v) = i\pi E[(E_v + E_I)/\hbar - \omega_{fg}] S^{(2)}(\omega_{fg}) \quad (3)$$

and

$$A_{\text{near-res}}^{(2+1)}(E_v) = -\wp \int_{-\infty}^{+\infty} (1/\Delta) E[(E_v + E_I)/\hbar - \omega_{fg} - \Delta] \times S^{(2)}(\omega_{fg} + \Delta) d\Delta, \quad (4)$$

with

$$S^{(2)}(\Omega) = \int_{-\infty}^{+\infty} E(\omega) E(\Omega - \omega) d\omega, \quad (5)$$

where  $E(\omega)$  is the Fourier transform of  $E(t)$  with  $E(\omega) = A(\omega)\exp[i\Phi(\omega)]$ ,  $A(\omega)$  and  $\Phi(\omega)$  are the spectral amplitude and phase in the frequency domain, respectively,  $\wp$  is the Cauchy's principal-value operator, and  $\Delta$  is the detuning of the nonresonant two-photon absorption. The term  $A_{\text{on-res}}^{(2+1)}(E_v)$  is the on-resonant component that interferes all on-resonant three-photon excitation pathways ( $\Delta = 0$ ) with the frequencies of  $\omega$ ,  $\omega_{fg} - \omega$ , and  $(E_v + E_I)/\hbar - \omega_{fg}$ , while the term  $A_{\text{near-res}}^{(2+1)}(E_v)$  is the near-resonant component that interferes all other near-resonant three-photon excitation pathways ( $\Delta \neq 0$ ) with the frequencies of  $\omega$ ,  $\omega_{fg} - \omega + \Delta$ , and  $(E_v + E_I)/\hbar - \omega_{fg} - \Delta$ , and so  $P^{(2+1)}(E_v)$  is the result of both the inter- and intragroup interferences involving on- and near-resonant three-photon excitation pathways. The different excitation pathways of on- and near-resonant three-photon ionization processes are presented in Fig. 1(a).

As can be seen from Eqs. (2)–(5), the on-resonant term  $A_{\text{on-res}}^{(2+1)}(E_v)$  is proportional to  $S^{(2)}(\omega_{fg})$ , corresponding to the nonresonant two-photon transition amplitude from the states  $|g\rangle$  to  $|f\rangle$ . It is easy to verify that  $S^{(2)}(\omega_{fg})$  is the maximal value for the transform-limited (unshaped) laser pulse [i.e.,  $\Phi(\omega) = 0$ ] or the shaped laser pulse with antisymmetric spectral phase distribution around the two-photon transition frequency  $\omega_{fg}/2$  [i.e.,  $\Phi(\omega_{fg}/2 + \delta) = -\Phi(\omega_{fg}/2 - \delta)$ ], and other spectral phase distributions will reduce and even eliminate it. Thus the on-resonant contribution  $|A_{\text{on-res}}^{(2+1)}(E_v)|^2$  can be suppressed but cannot be enhanced. However, the near-resonant term  $A_{\text{near-res}}^{(2+1)}(E_v)$  integrates over both positive ( $\Delta > 0$ ) and negative ( $\Delta < 0$ ) components, and therefore the transform-limited laser pulse induces a destructive interference in these near-resonant three-photon excitation pathways. By rationally designing the spectral phase distribution, the near-resonant contribution  $|A_{\text{near-res}}^{(2+1)}(E_v)|^2$  can be enhanced by inducing a constructive interference instead of the destructive interference. Based on the above analysis, the spectral phase step modulation, which produces a phase inversion, can provide a perfect method to control the constructive or destructive interferences in both on- and near-resonant components  $A_{\text{on-res}}^{(2+1)}(E_v)$  and  $A_{\text{near-res}}^{(2+1)}(E_v)$  and consequently the total  $P^{(2+1)}(E_v)$ . This simple spectral phase modulation is schematically shown in Fig. 1(b), where  $\alpha$  and  $\beta$  represent the phase step position and modulation depth, respectively. The phase step modulation is characterized by a phase jump from  $-\beta/2$  to  $\beta/2$  at the step position  $\alpha$ . In real experiment, this phase step modulation can be obtained by a programmable  $4f$ -configuration zero-dispersion pulse shaper combined with a one-dimensional liquid-crystal spatial light modulator [32], and has been successfully utilized to control the multiphoton-absorption or -ionization process [21,33].

We utilize the cesium (Cs) atom as our study system, and the states  $|6s\rangle$  and  $|9s\rangle$  are used as the ground state  $|g\rangle$  and the excited state  $|f\rangle$ , respectively. The transition frequency from the states  $|6s\rangle$  to  $|9s\rangle$  is  $\omega_{9s,6s} = 26910 \text{ cm}^{-1}$ , and the ionization energy is  $E_I = 3.89 \text{ eV}$ , corresponding to the frequency of  $31375 \text{ cm}^{-1}$ . The laser central frequency is set to be  $\omega_L = \omega_{9s,6s}/2 = 13455 \text{ cm}^{-1}$  and the laser spectral bandwidth (full width at half maximum) is set to be  $\Delta\omega = 300 \text{ cm}^{-1}$ . Figure 2 shows the normalized  $(2+1)$  REMPI-PS signals  $P^{(2+1)}(E_v)$  induced by the unshaped laser pulse (a) and the shaped laser pulse with the step position  $\alpha = 13455 \text{ cm}^{-1}$  and the modulation depth  $\beta = \pi$  (green solid lines), and both the on-resonant contribution  $|A_{\text{on-res}}^{(2+1)}(E_v)|^2$  (red dashed lines) and the near-resonant contribution  $|A_{\text{near-res}}^{(2+1)}(E_v)|^2$  (blue dotted lines) are also shown together. All data are normalized by the peak value of  $P^{(2+1)}(E_v)$  excited by the transform-limited laser pulse, and hereafter the same method is employed. One can see from Fig. 2(a) that  $|A_{\text{on-res}}^{(2+1)}(E_v)|^2$  dominates the total three-photon ionization process, i.e.,  $|A_{\text{on-res}}^{(2+1)}(E_v)|^2 \gg |A_{\text{near-res}}^{(2+1)}(E_v)|^2$  and  $|A_{\text{on-res}}^{(2+1)}(E_v)|^2 \approx P^{(2+1)}(E_v)$ . It is noteworthy that  $|A_{\text{near-res}}^{(2+1)}(E_v)|^2$  at the kinetic energy of  $E_v = 1.1146 \text{ eV}$  is completely suppressed, which is due to the completely destructive interference between the positive ( $\Delta > 0$ ) and negative ( $\Delta < 0$ ) components in these near-resonant three-photon excitation pathways [see Eq. (4)]. By the spectral phase step modulation, as shown in Fig. 2(b),  $|A_{\text{on-res}}^{(2+1)}(E_v)|^2$  is not affected because of the antisymmetric spectral phase distribution, while  $|A_{\text{near-res}}^{(2+1)}(E_v)|^2$  is greatly enhanced at the kinetic energy of

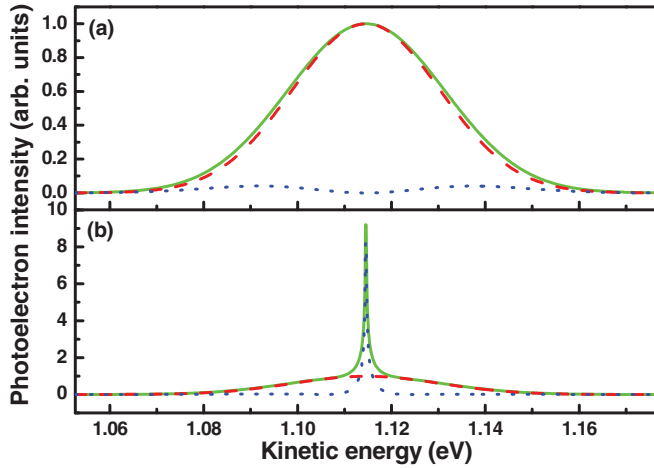


FIG. 2. (Color online) Normalized REMPI-PS signals  $P^{(2+1)}(E_v)$  in Cs atom induced by the unshaped laser pulse (a) and the shaped laser pulse with the step position  $\alpha = 13455 \text{ cm}^{-1}$  and modulation depth  $\beta = \pi$  (b) (green solid lines), together with the on-resonant contribution  $|A_{\text{on-res}}^{(2+1)}(E_v)|^2$  (red dashed lines) and the near-resonant contribution  $|A_{\text{near-res}}^{(2+1)}(E_v)|^2$  (blue dotted lines).

$E_v = 1.1146 \text{ eV}$  due to the constructive interference instead of the destructive interference, which results in the corresponding enhancement of  $P^{(2+1)}(E_v)$ , and the position of the maximal enhancement  $E_v^{\text{max}}$  and the phase step position  $\alpha$  exist in the relation of  $E_v^{\text{max}} = \hbar(\omega_{9s,6s} + \alpha) - E_I$ . Moreover, it can also be seen from Fig. 2(b) that the strong enhancement of  $P^{(2+1)}(E_v)$  at a given kinetic energy  $E_v$  will lead to the great narrowing of the photoelectron spectroscopy.

For the spectral phase modulation with the modulation depth  $\beta = \pi$ , i.e.,  $\Phi(\omega) = 0$  or  $\pi$ , the shaped laser field  $E(\omega)$  is a positive or negative real number for any  $\omega$ , and the on-resonant term  $A_{\text{on-res}}^{(2+1)}(E_v)$  is an imaginary number, while the near-resonant term  $A_{\text{near-res}}^{(2+1)}(E_v)$  is a real number [see Eqs. (3) and (4)]; thus  $P(E_v)$  is the sum of the on-resonant contribution  $|A_{\text{on-res}}^{(2+1)}(E_v)|^2$  and the near-resonant contribution  $|A_{\text{near-res}}^{(2+1)}(E_v)|^2$  (see Fig. 2), i.e.,  $P^{(2+1)}(E_v) = |A_{\text{on-res}}^{(2+1)}(E_v)|^2 + |A_{\text{near-res}}^{(2+1)}(E_v)|^2$ . In other words,  $P^{(2+1)}(E_v)$  is only determined by the intragroup interferences within each of the on- and near-resonant excitation pathways, and without the intergroup interferences between the on- and near-resonant excitation pathways occur. By varying the modulation depth  $\beta$ , the shaped laser field  $E(\omega)$  is not longer a real number but a complex number, and  $P^{(2+1)}(E_v)$  is written as

$$P^{(2+1)}(E_v) = |A_{\text{on-res}}^{(2+1)}(E_v)|^2 + |A_{\text{near-res}}^{(2+1)}(E_v)|^2 + A_{\text{on-res}}^{(2+1)}(E_v)[A_{\text{near-res}}^{(2+1)}(E_v)]^* + [A_{\text{on-res}}^{(2+1)}(E_v)]^* A_{\text{near-res}}^{(2+1)}(E_v),$$

which is determined by both intra- and intergroup interferences involving the on- and near-resonant excitation pathways, and thus a higher enhancement of  $P^{(2+1)}(E_v)$  can be realized by properly controlling the modulation depth  $\beta$ . Figure 3 shows the normalized photoelectron intensity measured at the kinetic energy of  $E_v^{\text{meas}} = 1.1146 \text{ eV}$   $P^{(2+1)}(E_v^{\text{meas}})$  as the function of the phase modulation depth  $\beta$  for the phase step position  $\alpha = 13455 \text{ cm}^{-1}$  (green solid line), together

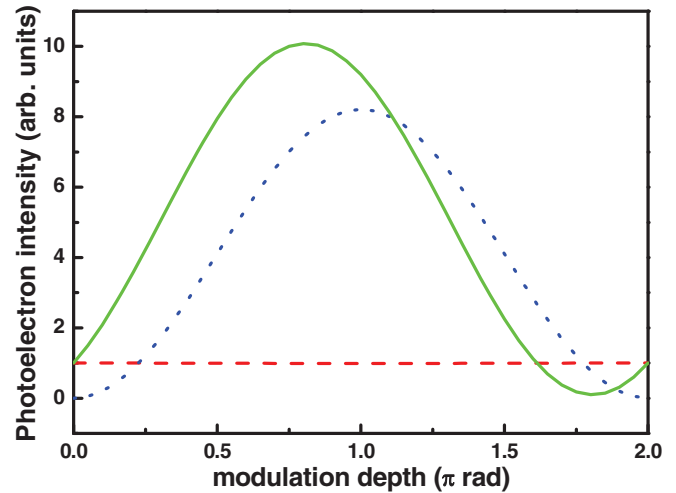


FIG. 3. (Color online) Normalized photoelectron intensity measured at the kinetic energy of  $E_v^{\text{meas}} = 1.1146 \text{ eV}$   $P^{(2+1)}(E_v^{\text{meas}})$  as the function of the phase modulation depth  $\beta$  for the phase step position  $\alpha = 13455 \text{ cm}^{-1}$  (green solid line), and also the on-resonant contribution  $|A_{\text{on-res}}^{(2+1)}(E_v^{\text{meas}})|^2$  (red dashed line) and the near-resonant contribution  $|A_{\text{near-res}}^{(2+1)}(E_v^{\text{meas}})|^2$  (blue dotted line) are presented.

with the on-resonant contribution  $|A_{\text{on-res}}^{(2+1)}(E_v^{\text{meas}})|^2$  (red dashed line) and the near-resonant contribution  $|A_{\text{near-res}}^{(2+1)}(E_v^{\text{meas}})|^2$  (blue dotted line). As can be seen, with the increase of  $\beta$ ,  $|A_{\text{on-res}}^{(2+1)}(E_v^{\text{meas}})|^2$  remains unchanged, while  $|A_{\text{near-res}}^{(2+1)}(E_v^{\text{meas}})|^2$  is maximally enhanced at  $\beta = \pi$ . In the range of  $\beta = 0$  and  $\pi$ , between on- and near-resonant excitation pathways is constructive interference, and  $P^{(2+1)}(E_v^{\text{meas}}) > |A_{\text{on-res}}^{(2+1)}(E_v^{\text{meas}})|^2 + |A_{\text{near-res}}^{(2+1)}(E_v^{\text{meas}})|^2$ . However, in the range of  $\beta = \pi$  and  $2\pi$ , between on- and near-resonant excitation pathways is destructive interference, and  $P^{(2+1)}(E_v^{\text{meas}}) < |A_{\text{on-res}}^{(2+1)}(E_v^{\text{meas}})|^2 + |A_{\text{near-res}}^{(2+1)}(E_v^{\text{meas}})|^2$ . Consequently,  $P^{(2+1)}(E_v^{\text{meas}})$  is maximally enhanced at  $\beta = 0.8\pi$  and maximally suppressed at  $\beta = 1.8\pi$ .

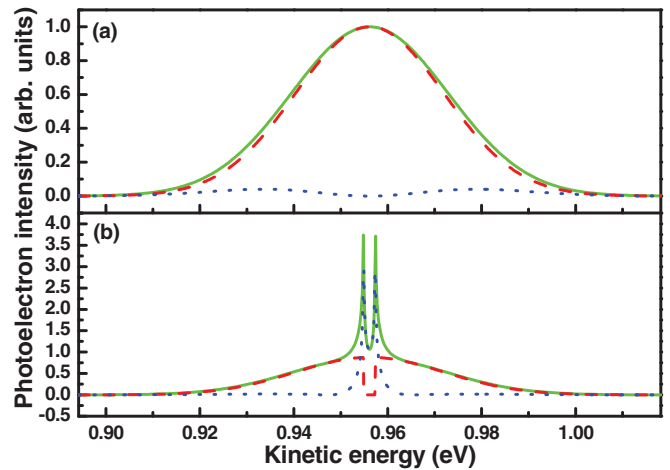


FIG. 4. (Color online) Normalized REMPI-PS signals  $P^{(2+1)}(E_v)$  in Cs atom induced by the unshaped laser pulse (a) and the shaped laser pulse with the step position  $\alpha = 13029 \text{ cm}^{-1}$  and modulation depth  $\beta = \pi$  (b) (green solid lines), and the on-resonant contribution  $|A_{\text{on-res}}^{(2+1)}(E_v)|^2$  (red dashed lines) and the near-resonant contribution  $|A_{\text{near-res}}^{(2+1)}(E_v)|^2$  (blue dotted lines) are also shown.

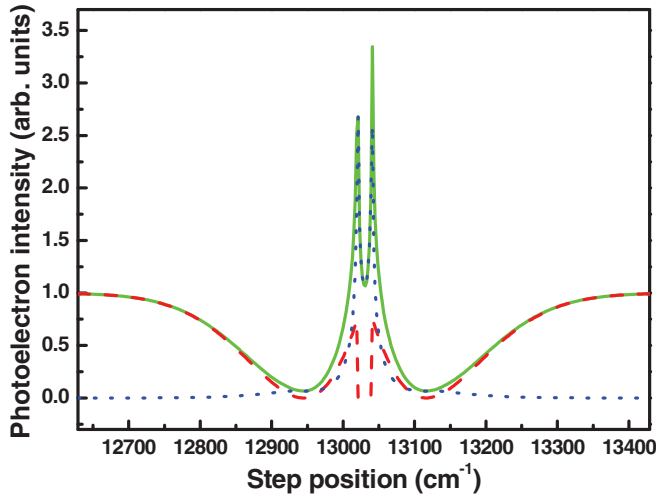


FIG. 5. (Color online) Normalized photoelectron intensity measured at the kinetic energy of  $E_v^{\text{meas}} = 0.9562$  eV  $P^{(2+1)}(E_v^{\text{meas}})$  as the function of the phase step position  $\alpha$  for the modulation depth  $\beta = \pi$  (green solid line), together with the on-resonant contribution  $|A_{\text{on-res}}^{(2+1)}(E_v^{\text{meas}})|^2$  (red dashed line) and the near-resonant contribution  $|A_{\text{near-res}}^{(2+1)}(E_v^{\text{meas}})|^2$  (blue dotted line).

As shown in Fig. 3, the shaped laser pulse with the spectral phase step modulation can enhance and narrow the REMPI-PS signal, and the maximal enhancement is obtained at the kinetic energy of  $E_v^{\text{max}} = \hbar(\omega_{fg} + \alpha) - E_I$ , which is correlated with the excited state  $|f\rangle$ ; thus a high-resolution REMPI-PS can be obtained when multiple excited states are simultaneously excited and ionized. We consider the excited state  $|7d\rangle$  of the Cs atom that involves two fine levels  $|7d_{1/2}\rangle$  and  $|7d_{3/2}\rangle$  with the transition frequencies of 26 048 and 26 068  $\text{cm}^{-1}$ , and their frequency separation is only 20  $\text{cm}^{-1}$ . We tune the laser central frequency to 26 058  $\text{cm}^{-1}$  and keep the spectral bandwidth of 300  $\text{cm}^{-1}$ . Figure 4 shows the normalized  $(2+1)$  REMPI signals  $P^{(2+1)}(E_v)$  in Cs atom induced by the unshaped laser pulse (a) and the shaped laser pulse with the step position  $\alpha = 13\,029$   $\text{cm}^{-1}$  and the modulation depth  $\beta = \pi$  (b) (green solid lines), and the contributions of the on-resonant component  $|A_{\text{on-res}}^{(2+1)}(E_v)|^2$  (blue dashed lines) and the near-resonant component  $|A_{\text{near-res}}^{(2+1)}(E_v)|^2$  (red dotted lines) are also presented. By the simple pulse shaping,  $|A_{\text{on-res}}^{(2+1)}(E_v)|^2$  for the two excited states  $|7d_{1/2}\rangle$  and  $|7d_{3/2}\rangle$  is indistinguishable, while  $|A_{\text{near-res}}^{(2+1)}(E_v)|^2$  is completely distinguishable [see Fig. 4(b)], and therefore two distinct narrowband peaks in  $P^{(2+1)}(E_v)$  are observed at the kinetic energies of  $E_v = 0.9548$

and 0.9574 eV, but only a single broadband peak is observed for the transform-limited laser pulse [see Fig. 4(a)]. Obviously, the spectral phase step modulation can provide an excellent method to obtain the high-resolution REMPI-PS and the excited-state structure in atomic and molecular systems.

Since the enhancement position of the REMPI-PS signal is determined by the phase step position  $\alpha$ , an alternative way to achieve the high-resolution REMPI-PS is measuring the photoelectron intensity at a given kinetic energy  $E_v^{\text{meas}}$  by scanning the step position  $\alpha$ . Figure 5 shows the normalized photoelectron intensity measured at the kinetic energy of  $E_v^{\text{meas}} = 0.9562$  eV  $P^{(2+1)}(E_v^{\text{meas}})$  as the function of the phase step position  $\alpha$  for the modulation depth  $\beta = \pi$  (green solid line), together with the contributions of the on-resonant component  $|A_{\text{on-res}}^{(2+1)}(E_v^{\text{meas}})|^2$  (blue dashed line) and the near-resonant component  $|A_{\text{near-res}}^{(2+1)}(E_v^{\text{meas}})|^2$  (red dotted line). Similarly,  $|A_{\text{near-res}}^{(2+1)}(E_v^{\text{meas}})|^2$  shows two narrowband peaks at the step positions of  $\alpha = 13\,021$  and  $13\,041$   $\text{cm}^{-1}$ , and therefore two distinct peaks in  $P^{(2+1)}(E_v^{\text{meas}})$  are observed at the same step positions. Based on the relation of  $E_v^{\text{meas}} = \hbar(\omega_{7d,6s} + \alpha) - E_I$ , and  $E_v^{\text{meas}}$  and  $\alpha$  are known from Fig. 6,  $\omega_{7d,6s}$  can be calculated. That is to say, the energy-level diagram of the two excited states can be accurately determined. In addition, one can see that the separation of two narrowband peaks (20  $\text{cm}^{-1}$ ) is exactly equal to the frequency difference of the two excited states, and therefore this can be used to determine the energy separation of the excited states.

In summary, we have demonstrated that, based on our theoretical model by perturbation theory, the  $(2+1)$  REMPI-PS signal in Cs atom can be greatly enhanced and narrowed due to the inter- and intragroup interferences involving on- and near-resonant three-photon excitation pathways by a spectral phase step modulation, and therefore a high-resolution REMPI-PS and fine energy-level diagram of the excited states can be obtained when multiple excited states are simultaneously excited and ionized. Since the enhancement and narrowing is general behavior of any quantum system around resonance, our theoretical scheme can be further applied to control the photoelectron spectroscopy in those more complex resonance-enhanced multiphoton-ionization processes. These theoretical results are also expected to serve as a basis for future extension to the molecular system.

#### ACKNOWLEDGMENTS

This work was partly supported by National Natural Science Fund (No. 11004060, No. 11027403, and No. 51132004) and Shanghai Rising-Star Program (No. 12QA1400900).

- [1] D. M. Neumark, *Annu. Rev. Phys. Chem.* **52**, 255 (2001).
- [2] A. Stolow, *Annu. Rev. Phys. Chem.* **54**, 89 (2003).
- [3] A. Stolow, *Int. Rev. Phys. Chem.* **22**, 377 (2003).
- [4] A. Stolow, A. E. Bragg, and D. M. Neumark, *Chem. Rev.* **104**, 1719 (2004).
- [5] M. Wollenhaupt, V. Engel, and T. Baumert, *Annu. Rev. Phys. Chem.* **56**, 25 (2005).

- [6] K. L. Ishikawa and K. Ueda, *Phys. Rev. Lett.* **108**, 033003 (2012).
- [7] J. Zhang, C. Harthcock, and W. Kong, *J. Phys. Chem. A* **116**, 1551 (2012).
- [8] C. Schröter, K. Kosma, and T. Schultz, *Science* **333**, 1011 (2011).
- [9] J. Zhang, C. Harthcock, F. Y. Han, and W. Kong, *J. Chem. Phys.* **135**, 244306 (2011).

- [10] Y. Hikosaka *et al.*, *Phys. Rev. Lett.* **105**, 133001 (2010).
- [11] L. Shen, B. L. Zhang, and A. G. Suits, *J. Phys. Chem. A* **114**, 3114 (2010).
- [12] F. Lépine, S. Zamith, A. de Snaijer, C. Bordas, and M. J. J. Vrakking, *Phys. Rev. Lett.* **93**, 233003 (2004).
- [13] J. Wassaf, V. Vénier, R. Taïeb, and A. Maquet, *Phys. Rev. Lett.* **90**, 013003 (2003).
- [14] T. A. Barckholtz, D. E. Powers, T. A. Miller, and B. E. Bursten, *J. Am. Chem. Soc.* **121**, 2576 (1999).
- [15] H. Park and R. N. Zare, *J. Chem. Phys.* **99**, 6537 (1993); **104**, 4568 (1996); **106**, 2239 (1997).
- [16] J. A. Davies, K. L. Reid, M. Towrie, and P. Matousek, *J. Chem. Phys.* **117**, 9099 (2002).
- [17] C. J. Hammond and K. L. Reid, *Phys. Chem. Chem. Phys.* **10**, 6762 (2008).
- [18] K. L. Reid, *Int. Rev. Phys. Chem.* **27**, 607 (2008).
- [19] M. Shapiro and P. W. Brumer, *Principles of the Quantum Control of Molecular Processes* (Wiley-Interscience, Hoboken, 2003).
- [20] S. A. Rice and M. Zhao, *Optical Control of Molecular Dynamics* (Wiley-VCH, New York, 2000).
- [21] M. Wollenhaupt, T. Bayer, N. V. Vitanov, and T. Baumert, *Phys. Rev. A* **81**, 053422 (2010).
- [22] M. Wollenhaupt, A. Präkelt, C. Sarpe-Tudoran, D. Liese, T. Bayer, and T. Baumert, *Phys. Rev. A* **73**, 063409 (2006).
- [23] M. Wollenhaupt, A. Präkelt, C. Sarpe-Tudoran, D. Liese, T. Bayer, and T. Baumert, *Appl. Phys. B* **82**, 183 (2006).
- [24] M. Wollenhaupt, A. Präkelt, C. Sarpe-Tudoran, D. Liese, and T. Baumert, *J. Opt. B* **7**, S270 (2005).
- [25] M. Krug, T. Bayer, M. Wollenhaupt, C. Sarpe-Tudoran, T. Baumert, S. S. Ivanov, and N. V. Vitanov, *New J. Phys.* **11**, 105051 (2009).
- [26] S. Zhang, H. Zhang, T. Jia, Z. Wang, and Z. Sun, *J. Phys. B* **43**, 135401 (2010).
- [27] S. Zhang, C. Lu, T. Jia, J. Qiu, and Z. Sun, *J. Chem. Phys.* **137**, 174301 (2012).
- [28] S. Zhang, C. Lu, T. Jia, and Z. Sun, *Phys. Rev. A* **86**, 012513 (2012).
- [29] S. Zhang, C. Lu, T. Jia, J. Qiu, and Z. Sun, *Phys. Rev. A* **86**, 043433 (2012).
- [30] C. Meier and V. Engel, *Phys. Rev. Lett.* **73**, 3207 (1994).
- [31] D. Meshulach and Y. Silberberg, *Phys. Rev. A* **60**, 1287 (1999).
- [32] A. M. Weiner, *Rev. Sci. Instrum.* **71**, 1929 (2000).
- [33] S. Zhang, H. Zhang, Y. Yang, T. Jia, Z. Wang, and Z. Sun, *J. Chem. Phys.* **132**, 094503 (2010).